Corals concentrate dissolved inorganic carbon to facilitate calcification

Nicola Allison[1]*, Itay Cohen[2], Adrian A. Finch[1], Jonathan Erez[3], Alexander W. Tudhope[4] and EIMF[5]

[1] Department of Earth Sciences, University of St Andrews, Irvine Building, North Street, St Andrews, Fife KY16 9AL, UK.

[2] The Interuniversity Institute of Eilat, P.O.B 469, Eilat 88103, Israel.

[3] The Institute of Earth Sciences, The Hebrew University of Jerusalem, Jerusalem 91904, Israel.

[4] School of Geosciences, Grant Institute, University of Edinburgh, Edinburgh EH9 3JW, UK

[5] Edinburgh Ion Microprobe Facility, Grant Institute, University of Edinburgh, Edinburgh EH9 3JW, UK

*** corresponding author**

Email: na9@st-andrews.ac.uk

Fax: +44 1334 463949

Abstract

The sources of dissolved inorganic carbon (DIC) used to produce scleractinian coral skeletons are not understood. Yet this knowledge is essential for understanding coral biomineralization and assessing the potential impacts of ocean acidification on coral reefs. Here we use skeletal boron geochemistry to reconstruct the DIC chemistry of the coral calcification fluid. We show that corals concentrate DIC at the calcification site substantially above seawater values and that bicarbonate contributes a significant amount of the DIC pool used to build the skeleton. Corals actively increase the pH of the calcification fluid, decreasing the proportion of DIC present as CO_2 and creating a diffusion gradient favoring the transport of molecular CO_2 from the overlying coral tissue into the calcification site. Coupling the increases in calcification fluid pH and [DIC] yields high ECF [CO_3^{2}] and induces high aragonite saturation states, favorable to the precipitation of the skeleton.

Neither the sources[1] nor species[2,3] of dissolved inorganic carbon (DIC) used during coral calcification are understood. The aragonite skeleton precipitates from an extracellular calcification fluid (ECF) enclosed in a semi-isolated space between the skeleton and the overlying coral tissue. The DIC utilized to form the coral skeleton is derived from seawater and from an internal DIC pool[1,4]. An active bicarbonate transporter has not been ruled out in coral, but dual radiolabelling studies suggest that this is not the source of additional carbon[4]. The isotopically light carbon and oxygen composition of coral skeletons suggests that molecular CO_2 may act as the source of internal DIC[5]. Understanding the sources of skeletal carbon is key to the accurate prediction of the effects of increasing [DIC] in seawater (ocean acidification) and for the correct interpretation of $\delta^{18}O$ and $\delta^{13}C$ coral based palaeoenvironmental records.

We analysed the B/Ca and B isotope ratio ($\delta^{11}B$) of coral aragonite to reconstruct the DIC chemistry of the coral ECF. Dissolved boron in seawater occurs primarily as boric acid, $B(OH)_3$, and borate, $B(OH)_4^-$, and speciation is controlled by ambient pH[6]. Borate is selectively incorporated

43 into aragonite[7], presumably substituting for CO_3^{2-} in the lattice. There are no known active transport
44 mechanisms for boron in corals and we assume that dissolved boron is transported to the ECF in
45 seawater. Seawater transport to the ECF is a passive process[8] and as such the transport rate is likely
46 to be constant. At equilibrium, $B(OH)_3$ is enriched in ^{11}B compared to $B(OH)_4^-$ [9], hence the $\delta^{11}B$ of
47 coral aragonite reflects ECF pH. Skeletal [B] reflects both ECF pH and the concentration of the
48 DIC species competing with borate for inclusion in the carbonate[10].

49 Passive diffusion of $B(OH)_3$ across cell membranes[11] could potentially offset ECF $\delta^{11}B$ from
50 seawater values. However ECF pH estimates derived from skeletal $\delta^{11}B$ compare well with direct
51 characterizations using fluorescent probes, suggesting this effect is insignificant i.e. observed ECF
52 pH in *Stylophora pistillata* (8.69 and 8.36 in the light and dark) cultured at seawater pH 8.1[(12)] is in
53 excellent agreement with $\delta^{11}B$ of the same species cultured at pH 8.09 (24.8 ‰, equivalent to an
54 ECF pH of 8.55)[13], assuming that calcification is 3 times faster in the light than the dark[14]. A recent
55 suggestion that skeletal $\delta^{11}B$ ECF pH estimates may be offset to lower values than expected[15] is
56 based on a comparison of skeletal $\delta^{11}B$ and direct ECF pH measurements in the light only. ECF pH
57 is lower in the dark[16] and this likely accounts for the offset.

58 We used skeletal $\delta^{11}B$ to estimate ECF pH[17] and B/Ca to estimate the concentration of the
59 DIC species which co-precipitates with $B(OH)_4^-$. It is not clear if CO_3^{2-} or HCO_3^- ions are utilized
60 during coral aragonite precipitation[2,3]. We consider 3 scenarios: that $B(OH)_4^-$ co-precipitates with
61 CO_3^{2-} only (scenario 1), with HCO_3^- only (scenario 2) or with both CO_3^{2-} and HCO_3^- (scenario 3).
62 We estimated the $B(OH)_4^-/CO_3^{2-}$, $B(OH)_4^-/HCO_3^-$ and $B(OH)_4^-/(CO_3^{2-} + HCO_3^-)$ aragonite partition
63 coefficients from an estimate of the $\delta^{11}B$ and B/Ca of secondary aragonite cement in a fossil coral
64 coupled with alkalinity measurements of coral skeletal pore fluids[18]. We used our estimates of ECF
65 pH and co-precipitating DIC species to calculate the concentrations of the other carbonate system
66 variables in the ECF, namely all other DIC species and total alkalinity (TA). We show that the ECF
67 pH and DIC chemistry is significantly different from that of seawater and that bicarbonate

contributes a significant amount of the DIC pool used to build the skeleton.

Results and discussion

Modern *Porites* spp. field corals.

We analysed 3 modern massive Porites spp. field corals from Oahu, Hawaii and Jarvis Island, South Pacific. Skeletal $\delta^{11}B$ ECF pH estimates (Figure 1, Table 1) confirm that corals actively increase the pH of the ECF above that of seawater[12,16]. The ECF composition reflects the balance of DIC inputs and outputs, namely seawater diffusion, molecular CO_2 invasion, proton extrusion and calcification (Figure 2). CO_2 invasion does not influence TA and the departure of ECF [TA] from seawater values reflects calcification (reduces [TA]) and proton extrusion (increases [TA]). Similarly, proton extrusion does not affect [DIC] and the departure of ECF [DIC] from seawater values reflects calcification (reduces [DIC]) and CO_2 invasion (increases [DIC]).

Under Scenario 1 (borate coprecipitates with CO_3^{2-}), the ECF has [DIC] and [TA] which are substantially lower than ambient seawater (Figure 1). Ca-ATPase activity has little effect on the [Ca] of the ECF[19] and in scenario 1, the aragonite saturation state (Ω) of the ECF (essentially a product of [Ca] and [CO_3^{2-}]) is ~3 and below that of seawater (Ω = ~4). It is implausible that the high calcification rates observed in tropical corals are attained with such an impoverished ECF and we reject this scenario.

Scenario 2 (borate co-precipitates with HCO_3^-) and scenario 3 (borate co-precipitates with both HCO_3^- and CO_3^{2-}) produce broadly similar results (Figure 1) as HCO_3^- is the most abundant carbon species (70-90%) over the observed ECF pH range. Proton pumping maintains ECF TA in the untreated corals well above seawater concentrations and [DIC] is up to double that of ambient seawater (Figure 1). ECF Ω in the untreated corals rises to 11-19, depending on coral and scenario, and facilitates rapid aragonite precipitation. These are both credible scenarios. Our observation, that borate co-precipitates with HCO_3^- in the aragonite lattice, indicates that a large proportion of

skeletal carbon is ultimately derived from the bicarbonate of the ECF. It is unknown if HCO_3^- deprotonates before or after binding to the aragonite[20] but the key point is that bicarbonate contributes to the DIC pool used during calcification.

Under scenarios 2 and 3 up to half of the DIC used in calcification does not come though the seawater transport pathway. The enzyme driven increase in ECF pH shifts the DIC equilibrium in favour of CO_3^{2-} at the expense of CO_2 and HCO_3^-, and creating a diffusion gradient favouring the diffusion of molecular CO_2 from the overlying coral tissue into the ECF[21]. We conclude that this is a likely source of the additional skeletal carbon. This interpretation is supported by geochemical and modeling studies that indicate a substantial proportion of coral aragonite is derived from an isotopically light (with respect to carbon and oxygen) molecular CO_2 source[5,21]. We note that ECF $[CO_2]$ in the field corals is significantly below that of seawater. Either CO_2 diffusion rate into the ECF is rate limited or the mean $[CO_2]$ in the overlying coral tissue is reduced below that of seawater.

Cultured *Pocillopora damicornis*

To investigate this further, we analysed cultured colonies of the branching coral, *Pocillopora damicornis,* some of which were incubated with the Ca-ATPase enzyme inhibitor, ruthenium red[22]. Ca-ATPase pumps Ca^{2+} into and H^+ out of the ECF and increases ECF pH[19]. Ruthenium red solutions absorb light from 430-615 nm however the collective evidence suggests that the chemical reduces coral calcification rate by directly inhibiting Ca-ATPase rather than by inhibiting zooxanthellar photosynthesis[22].

This experiment was designed to explore the response of ECF DIC chemistry to changes in ECF pH and all the cultured colonies were grown (by asexual budding and division) from branches of a single parent colony i.e. all colonies were genetically identical. We do not infer that the ECF DIC chemistry of the cultured colonies is representative of this coral species in the field. We

cultured duplicate corals in each treatment and in the solvent control and a single colony in the seawater control. We model the ECF DIC chemistry for each coral colony separately (Figute 3). Inhibition of Ca-ATPase decreased skeletal $\delta^{11}B$ (and ECF pH) in the high ruthenium red treatment compared to both the seawater and DMSO controls.

However there is little variation in reconstructed ECF [CO_2] despite the large ECF pH range observed in these specimens. To illustrate the relationships between ECF pH and DIC chemistry we plotted ECF [DIC] and Ω as a function of ECF pH and CO_2 assuming that CO_2 diffuses freely into the ECF maintaining equilibrium with an overlying CO_2 source (Figure 4). ECF DIC increases with increasing pH, reflecting the conversion of CO_2 to other DIC species at high pH and the diffusion of additional CO_2 into the ECF thereby concentrating DIC. Ω increases with increasing pH, reflecting the increase in ECF [CO_3^{2-}] with pH. The datasets from both the cultured and field corals indicate that ECF [CO_2] is ~third to half that in ambient seawater across all treatments. We are unable to determine if this reflects an equilibrium with the overlying CO_2 source or indicates a rate limitation on the diffusion of CO_2 into the ECF. We find a strong positive correlation between ECF aragonite saturation state and coral calcification rate (Figure 5) although we note that the rate dependence in coral is less than in aragonite inorganically precipitated at the same temperature i.e. doubling aragonite saturation state increases precipitation by x 1.5 in coral and x 5 in synthetic aragonite[23]. This is perhaps to be expected. Corals do not precipitate randomly but exert exquisite control over both the sites of precipitation and crystal morphology[24].

Our findings have implications for predicting the effects of ocean acidification on coral reefs. Although the ECF pH gradient facilitates the diffusion of CO_2 into the calcification site we find that ECF [CO_2] in all field corals is significantly below that of seawater. Ocean acidification decreases seawater pH but increases seawater [DIC] and [CO_2]. Understanding how these changes will impact both ECF pH and the diffusion of CO_2 into the coral ECF as a carbon concentration mechanism is key to interpreting current ocean acidification studies and predicting the effects of future scenarios.

Methods

Sample processing

For further details of field sites and coral culturing procedures see [17,22,25,26]. Cultured corals were originally collected from the Gulf of Eilat and were maintained in seawater at ambient salinity (40.6). Each culture experiment lasted for 5 days. Individual colonies were placed in flow through coral chambers at the start of day 1 and ruthenium red dissolved in dimethyl sulfoxide solution (DMSO) to a final concentration of 0.1% was added to the seawater supplied to the chambers at the start of day 2. A stable isotope tracer (^{42}Ca as $^{42}CaCO_3$) was added to the seawater at the same time as the inhibitor, allowing accurate identification of skeleton deposited in the presence of the inhibitor (if used) by SIMS. This tracer increased the seawater $^{42}Ca/^{44}Ca$ from 0.31 to ~0.40 and increased the [Ca] of seawater by ~0.2%. A DMSO control (0.1%) and a seawater control (with the addition of $^{42}CaCO_3$ only) were also tested. All treatments were tested in duplicate. Light and dark coral calcification rates were estimated each day[22] using the alkalinity anomaly technique[2].

Modern field and cultured corals were living when collected/sacrificed. Specimens were immersed in 3-4% sodium hypochlorate (I) solutions for ≥8 h with intermittent ultrasonic agitation to remove organic contamination, then rinsed repeatedly in distilled water and dried. Skeletal strips were sawn along the maximum growth axis of the field specimens, divided into 10-15 mmlengths and fixed to 25 mm round thin sections. Branch ends of cultured corals were fixed into 25 mm circular epoxy resin blocks (Epofix, Struers Ltd.). Sections and blocks were polished using silicon carbide papers (up to 4000 grade, lubricated with water) and polishing alumina (0.05 µm, suspended in water). Multiple SIMS analyses were evenly spaced across 1 year (Jarvis coral) and 2 years (both Hawaiian corals) of skeletal growth in the field corals. Annual growth bands were identified from X-ray radiographs in the Hawaiian corals and from unpublished $\delta^{13}C$ data, which exhibit a seasonal trend, in the Jarvis coral. No analyses were made in the outermost parts of the

168 field skeletons which contained the tissue layers of the corals. In the cultured corals, SIMS analyses
169 were sited on the outermost tips of the skeleton. Analyses which did not exhibit enhanced $^{42}Ca/^{44}Ca$
170 throughout the analysis were rejected. Sections were repolished between batches of analyses to
171 expose fresh areas for SIMS.
172
173 **$\delta^{11}B$ and B/Ca analyses**
174 Skeletal $\delta^{11}B$ and B/Ca were determined by secondary ion mass spectrometry (SIMS) in the
175 School of GeoSciences at the University of Edinburgh. The high spatial resolution of SIMS
176 (primary beam diameters = 25-40 µm) allows the selective analysis of both the primary coral
177 aragonite, avoiding contamination from secondary cements or microboring organisms, and the
178 small skeletal volumes deposited in the culture experiment. $\delta^{11}B$ in the Hawaiian and cultured
179 corals were analysed with a Cameca 1270 while the Jarvis coral was analysed with a Cameca 4f.
180 One coral (Hawaii 1) had also previously been analysed using the Cameca 4f[17] and there is
181 excellent agreement in standardized $\delta^{11}B$ estimates between the 2 instruments (within 0.4‰,
182 equivalent to a pH of 0.03). B/Ca was determined using the Cameca 4f. Cultured coral analyses
183 were normalized to multiple daily analyses of a *Porites* spp. coral standard ($\delta^{11}B$ = 24.8‰, B/Ca =
184 0.364 mmol mol^{-1} [27]). The standard deviation (1σ) of bracketed standard analyses (n= 13-19) each
185 day was $\delta^{11}B$ = 1.7‰ and B/Ca = 9%. Field coral analyses were normalized to the same *Porites*
186 spp. standard but a more homogenous *Desmophyllum* spp. cold water coral chip was used to check
187 for instrumental drift within and between days. The standard deviation (1σ) of bracketed standard
188 analyses (n= 15-27) each day was $\delta^{11}B$ = 1.2‰ and B/Ca = 2%. The precision (2σ) of the Porites
189 spp. standard in each session was equivalent to ±0.02 pH units and ±3% B/Ca.
190
191 **Estimation of partition coefficients**
192 We estimated $B(OH)_4^-/CO_3^{2-}$, $B(OH)_4^-/HCO_3^-$ and $B(OH)_4^-/(CO_3^{2-}+HCO_3^-)$ aragonite partition

coefficients from $\delta^{11}B$ and B/Ca analyses of secondary aragonite cement in a Hawaiian fossil coral dated to 13.4ky. We used $\delta^{11}B$ to estimate coral pore fluid pH and assumed a porewater TA of 2162 ± 78 µmol kg^{-1} (n=4) based on repeat measurements of skeletal pore fluids in a modern coral[18]. Porewater [Ca] is similar to adjacent reefwaters (within 5%)[18] and we assume that porewater [B] is the same as seawater (416 µmol kg^{-1}) at the collection site of the fossil coral. We estimated $B(OH)_4^-/CO_3^{2-}$, $B(OH)_4^-/HCO_3^-$ and $B(OH)_4^-/(CO_3^{2-}+HCO_3^-)$ aragonite partition coefficients of 0.283, 4.51 and 4.79 all x 10^{-3} respectively (Supplementary Table 1).

Calculation of ECF DIC parameters

The equilibrium constant, K_B, and its pK_B value were calculated[28] from the known temperatures and salinity of the field sites and culture seawater. Mean annual salinity and temperature at the Jarvis and Hawaii reef sites are 35.5 and 27.4°C[29] and 35.0 and 25.0°C[17] respectively. Salinity and temperature in the culture system were 40.6 and 25.0°C[22].

ECF pH was estimated from skeletal $\delta^{11}B$:

$$pH_{ECF} = pK_B - \log\left(-\frac{\delta^{11}B_{ECF} - \delta^{11}B_{aragonite}}{\delta^{11}B_{ECF} - \alpha_B\,\delta^{11}B_{aragonite} - 1000(\alpha_B - 1)}\right) \quad (1)$$

using the empirically-determined α_B (=1.0272)[9] and assuming that the $\delta^{11}B_{ECF}$ is the same as seawater (39.5‰).

We assumed that $[B]_{ECF}$ is the same as seawater i.e.

416 x S/35 µmol kg^{-1}, where S = salinity[28]. (2)

We used pH_{ECF} to estimate the $[B(OH)_4^-]_{ECF}$:

$$K^*_B = \frac{[H^+]_{ECF}\,[B(OH)_4^-]_{ECF}}{[B(OH)_3]_{ECF}} \quad (3)$$

$B/Ca_{aragonite}$ equates to $B/CO_3^{2-}{}_{aragonite}$ as Ca and C are equimolar in $CaCO_3$. We used $[B(OH)_4^-]_{ECF}$, $B/Ca_{aragonite}$ and the relevant B/(co-precipitating DIC species) partition coefficient to estimate the concentration of the DIC species co-precipitating with $B(OH)_4^-$ in the ECF. e.g.

$$\text{In scenario 1: } B/Ca_{aragonite} = K_D B(OH)_4^-/CO_3^{2-} \times \frac{[B(OH)_4^-]_{ECF}}{[CO_3^{2-}]_{ECF}} \quad (4)$$

$$\text{In scenario 2: } B/Ca_{aragonite} = K_D B(OH)_4^-/HCO_3^- \times \frac{[B(OH)_4^-]_{ECF}}{[HCO_3^-]_{ECF}} \quad (5)$$

We used pH_{ECF} and the concentration of the DIC species co-precipitating with $B(OH)_4^-$ in the ECF (i.e. $[CO_3^{2-}]_{ECF}$ in scenario 1, $[HCO_3^-]_{ECF}$ in scenario 2 etc) to estimate all the other parameters in the ECF DIC system. DIC system parameters were calculated using CO_2sys.xls[30] using acidity constants K_1 and K_2 from Roy et al., 1993 (ref 31) and $KHSO_4$ from Dickson (1990, ref 32). ECF Ω was calculated using ECF $[CO_3^{2-}]$ and assuming that ECF $[Ca^{2+}]$ was similar to seawater[19].

References

1. Erez, J. Vital effect on the stable-isotope composition seen in foraminifera and coral skeletons. *Nature* **273**, 199-202 (1978).
2. Schneider, K. & Erez, J. The effect of carbonate chemistry on calcification and photosynthesis in the hermatypic coral *Acropora eurystoma*. *Limnol.. Oceanogr.*, **51**, 1284-1293, (2006).
3. Jury, C. P., Whitehead, R. F. & Szmant, A. M. Effects of variations in carbonate chemistry on the calcification rates of *Madracis auretenra* (= *Madracis mirabilis* sensu Wells, 1973): bicarbonate concentrations best predict calcification rates. *Global Change Biol.*. **16**:1632-1644 (2010).
4. Furla, P., Galgani, I., Durand, I. & Allemand, D. Sources and mechanisms of inorganic carbon

transport for coral calcification and photosynthesis. *J. Exp. Biol*., **203**, 3445-3457 (2000).

5. Weber, J. N. & Woodhead, P. M. J. Carbon and oxygen isotope fractionation in the skeletal carbonate of reef-building corals, *Chem. Geol.,* **6**, 93-117 (1970).
6. Hemming, N. G. & Hanson, G. N. Boron isotopic composition and concentration in modern marine carbonates. *Geochim. Cosmochim. Acta*, **56**, 537-543 (1992).
7. Sen, S., Stebbins, J. F., Hemming, N. G. & Ghosh, B. Coordination environments of B-impurities in calcite and aragonite polymorphs - a B-11 mas NMR-study. *Am. Mineralogist*, **79**, 819-825 (1994).
8. Tambutte, E., et al. Calcein labelling and electrophysiology: insights on coral tissue permeability and calcification*Proc. Royal Soc. B*, **279**, 19-27 (2012).
9. Klochko, K., Kaufman, A. J., Yao, W. S., Bryne, R. H. & Tossell, J. A. Experimental measurement of boron isotope fractionation in seawater. *Earth Planet. Sci. Lett*., **248**, 276-285 (2006).
10. Allen, K. A., Honisch, B., Eggins, S. M. & Rosenthal Y. Environmental controls on B/Ca in calcite tests of the tropical planktic foraminifer species *Globigerinoides ruber* and *Globigerinoides sacculifer*. *Earth Planet. Sci. Lett.,* **351-352**, 270-280 (2012).
11. Dordas C. & Brown P. H. Permeability and mechanism of transport of boric acid across the plasma membrane of *Xenopus laevis* oocytes. *Biological Trace Element Res.,* **81,** 127-139 (2001).
12. Venn, A. A. et al. Impact of seawater acidification on pH at the tissue-skeleton interface and calcification in reef corals. *Proc. Natl. Acad. Sci.*, **110**, 1634-1639 (2012).
13. Krief, S. et al. Physiological and isotopic responses of scleractinian corals to ocean acidification. *Geochim. Cosmochim. Acta* **74**, 4988 – 5001 (2010).

14. Gattuso, J. P., Allemand, D. & Frankignoulle, M. Photosynthesis and calcification at cellular, organismal and community levels in coral reefs: A review on interactions and control by carbonate chemistry. *Am. Zool*., **39**, 160-183 (1999).
15. Gagnon, A. C. Coral calcification feels the acid. *Proc. Natl. Acad. Sci.*, **110**, 1567-1568 (2013).
16. Venn, A. A., Tambutte, E., Holcomb, M., Allemand, D.& Tambutte, S. Live tissue imaging shows reef corals elevate pH under their calcifying tissue relative to seawater. *PLoS ONE* **6**, e20013, (2011).
17. Allison, N., Finch, A. A. & EIMF. δ^{11}B, Sr, Mg and B in a modern Porites coral: the relationship between calcification site pH and skeletal chemistry. *Geochim. Cosmochim. Acta*, **74**, 1790-1800 (2010).
18. Enmar, R., et al. Diagenesis in live corals from the Gulf of Aqaba. I. The effect on paleo-oceanography tracers. *Geochim. Cosmochim. Acta*, **64**, 3123-3132 (2000).
19. Al-Horani, F. A., Al-Moghrabi, S. M. & de Beer, D. The mechanism of calcification and its relation to photosynthesis and respiration in the scleractinian coral *Galaxea fascicularis*. *Mar. Biol*., **142**, 419-426 (2003).
20. Adkins, J. F., Boyle, E. A., Curry, W. B. & Lutringer, A. Stable isotopes in deep-sea corals and a new mechanism for "vital effects" *Geochim. Cosmochim. Acta*, **67**, 1129-1143 (2003).
21. McConnaughey, T. A. Sub-equilibrium oxygen-18 and carbon-13 levels in biological carbonates: carbonate and kinetic models *Coral Reefs*, **22**, 316-327 (2003).
22. Allison, N. Cohen, I., Finch, A. A, Erez, J. & E.I.M.F. Controls on Sr/Ca and Mg/Ca in scleractinian corals: the effects of Ca-ATPase and transcellular Ca channels on skeletal chemistry *Geochim. Cosmochim.Acta*, **75**, 6350-6360 (2011).
23. Burton, E. A., & Walter, L. M. Relative precipitation rates of aragonite and Mg calcite from seawater**:** temperature or carbonate ion control *Geology*, **15**, 111-114 (1987).

24. Falini G. et al., Control of aragonite deposition in colonial corals by intra-skeletal macromolecules. *J. Struct. Biol*, **183**, 226-238 (2013).

25. Allison N. & Finch A. A. High resolution Sr/Ca records in modern *Porites lobata* corals: effects of skeletal extension rate and architecture *Geochem. Geophys. Geosyst*., **5**, Q05001 (2004).

26. Marriott, C. S., Henderson, G. M., Belshaw, N. S. & Tudhope A. W. Temperature dependence of δ^7Li, δ^{44}Ca and Li/Ca during growth of calcium carbonate. *Earth Planet. Sci Lett*., **222**, 615-624 (2004).

27. Kasemann, S. A., Schmidt, D. N., Bijma, J. & Foster, G. L. In situ boron isotope analysis in marine carbonates and its application for foraminifera and palaeo-pH. *Chem. Geol*., **260**, 138-147 (2009).

28. D.O.E. *Handbook f Methods for the Analysis of the Various Parameters of the Carbon Dioxide System in Seawater*. Department of Energy. A. G. Dickson & C. Goyet, eds. ORNL/CDIAC-74, Version 2 (1994).

29. Price, N. N., Martz, T. R., Brainard, R. E. & Smith, J. E. Diel variability in seawater pH relates to calcification and benthic community structure on coral reefs. *PLoSone*, **7**, e43843 (2012).

30. Pierrot, D. E. Lewis, D., & Wallace W. R. *MS Excel Program Developed for CO_2 System Calculations*. ORNL/CDIAC-105a, Carbon Dioxide Information Analysis Center, Oak Ridge National Laboratory, U.S. Department of Energy, Oak Ridge, Tennessee (2006).

31. Roy, R.N. et al.The dissociation constants of carbonic acid in seawater at salinities 5 to 45 and temperatures 0 to 45°C. *Mar. Chem*., **44**, 249-267 (1993).

32. Dickson, A. G., Standard potential of the reaction: AgCl2(s) + 1/2H2(g) = Ag(s) + HCl(aq), and the standard acidity constant of the ion HSO_4 in synthetic seawater from 273.15 to 318.15 K. *J. Chem. Thermodyn*. **22**, 113–127 (1990).

33. Fagan, K. E. & Mackenzie, F. T. Air–sea CO_2 exchange in a subtropical estuarine-coral reef system, Kaneohe Bay, Oahu, Hawaii. *Mar. Chem.*, **106**, 174-191 (2007).

Supplementary information is available in the online version of the paper.

Acknowledgements

This work was supported by the UK Natural Environment Research Council (awards NER/A/S/2003/00473 and NE/G015791/1 to NA and AF; NER/GR3/12021 to AWT). Participation of JE and IC of this study was supported by DFG project Trion and the Israel Science Foundation (grants 870/05 and 551/10). Access to the ion probe was provided by NERC Scientific Services.

Author contributions

NA, JE and AF designed the study. Field samples were collected by NA, AF and AWT. Coral culturing was performed by NA, IC and JE. SIMS was performed by NA and AF. All authors contributed to the analysis of the results and to the writing of the paper.

Additional Information

The authors declare no competing financial interests. Correspondence and requests for materials should be addressed to NA.

Figure legends

Figure 1. Geochemistry and reconstructed calcification fluid **DIC of *Porites* spp. field corals.** (a) extracellular calcification fluid (ECF) pH (from skeletal $\delta^{11}B$), (b) skeletal B/Ca and (c)

reconstructed ECF DIC system parameters. TA = total alkalinity, Ω = aragonite saturation state. Both $\delta^{11}B$ and B/Ca are normally distributed in each coral and error bars are 95% confidence limits (s.e.m.). Data are means of ≥99 B/Ca analyses and ≥40 $\delta^{11}B$ analyses with the exception of $\delta^{11}B$ in the Jarvis coral where only 12 analyses were made, note the larger confidence limits. DIC system errors are calculated from propagating 95% confidence limits in B/Ca and $\delta^{11}B$ analyses onto DIC system estimates. Horizontal lines denote seawater concentrations and are calculated from observations of pH and total alkalinity in Jarvis Island benthic reefwater[29] and DIC and total alkalinity in Hawaii reefwater[33].

Figure 2. Schematic summarising the processes affecting the DIC system in the coral calcification fluid. The DIC composition reflects the balance of inputs and outputs, namely seawater diffusion, molecular CO_2 invasion, proton extrusion and calcification.

Figure 3. Geochemistry and reconstructed calcification fluid DIC of cultured *P. damicornis* corals. (a) extracellular calcification fluid (ECF) pH (from skeletal $\delta^{11}B$), (b) skeletal B/Ca and (c) reconstructed ECF DIC system parameters. TA = total alkalinity, Ω = aragonite saturation state. Error bars are 95% confidence limits (s.e.m.). Cultured corals were exposed to ruthenium red (RR) dissolved in 0.1% DMSO and DMSO and seawater only controls (con.) were also analysed. Corals were analysed in duplicate (indicated by 1 or 2 annotation). 7-16 analyses were collected on each sample (Table 1) with the exceptions of RR 3.7 µM 2 and RR 5.3 µM 1 where only 2 and 1, respectively, credible $\delta^{11}B$ analysis (exhibiting the ^{42}Ca spike throughout the analysis) were obtained. Errors are calculated as for the field corals and horizontal lines denote seawater concentrations calculated from observations of pH and total alkalinity in the culture seawater[22].

Figure 4. Modelled relationships between calcification fluid pH and DIC parameters under a

range of CO_2 scenarios. (a) Extracellular calcification fluid (ECF) [DIC] and (b) ECF **aragonite saturation state** (Ω) increase with ECF pH, assuming that CO_2 readily diffuses into the calcification site, maintaining an equilibrium with an overlying [CO_2] ranging from that of ambient seawater to 1/8 of this. DIC calculations were made using CO_2 sys[30], assuming seawater T=25°C and S=40.6 i.e. the conditions in the culture seawater. Reconstructed DIC parameters under scenario 3 in the field and cultured corals are overlain on each graph. Field corals grew under different temperatures and salinities but this does not affect the interpretation of these graphs. Error bars are 95% confidence limits (s.e.m.) and in the case of ECF DIC are smaller than the heights of the symbols.

Figure 5. Correlation between reconstructed calcification fluid aragonite saturation state and colony calcification rate in the cultured corals. Aragonite saturation state (Ω) was calculated under scenario 3. Calcification rate is calculated from the mean calcification rate measured in the presence of the inhibitor, if used, as a proportion of the calcification rate observed on day 1, before the introduction of the inhibitor[22]..

Colony	B/Ca (mmol mol^{-1})	$\delta^{11}B$ (‰)	ECF pH_{total}
Porites spp. field corals			
Hawaii 1	0.296 ± 0.038 (n=144)	24.5 ± 1.4 (n=40)	8.53 ± 0.14 (n = 40)
Hawaii 2	0.328 ± 0.041 (n=129)	23.7 ± 1.9 (n=52)	8.48± 0.17 (n = 52)
Jarvis	0.341 ± 0.028 (n=99)	24.6 ± 2.4 (n=12)	8.51 ± 0.16 (n = 12)
Cultured *Pocillopora damicornis*			
Seawater control	0.345 ± 0.040 (n=13)	22.2 ± 1.6 (n=13)	8.33 ± 0.11 (n=13)
DMSO control 1	0.360 ± 0.030 (n=11)	22.3 ± 2.9 (n=9)	8.33 ± 0.20 (n=9)
DMSO control 2	0.397 ± 0.036 (n=11)	20.6 ± 1.5 (n=9)	8.21 ± 0.11 (n=9)
RR 3.7 µM 1	0.411 ± 0.047 (n=16)	19.3 ± 1.8 (n=7)	8.11 ± 0.15 (n=7)
RR 3.7 µM 2	0.430 ± 0.053 (n=8)	20.7 ± 2.1 (n=2)	8.22 ± 0.15 (n=2)
RR 5.3 µM 1	0.412 ± 0.035 (n=10)	16.8 (n=1)	7.89 (n=1)
RR 5.3 µM 2	0.433 ± 0.040 (n=12)	17.8 ±2.6 (n=8)	7.94 ± 0.32 (n=8)

Table 1. Measured B/Ca and $\delta^{11}B$ in each coral colony and ECF pH estimated from $\delta^{11}B$. Values are means ± standard deviation (1σ) of n measurements.

388

Figure 1. Geochemistry and reconstructed calcification fluid DIC of Porites spp. field corals. (a) extracellular calcification fluid (ECF) pH (from skeletal δ11B), (b) skeletal B/Ca and (c) reconstructed ECF DIC system parameters. TA = total alkalinity, Ω = aragonite saturation state. Both δ11B and B/Ca are normally distributed in each coral and error bars are 95% confidence limits (s.e.m.). Data are means of ≥99 B/Ca analyses and ≥40 δ11B analyses with the exception of δ11B in the Jarvis coral where only 12 analyses were made, note the larger confidence limits. DIC system errors are calculated from propagating 95% confidence limits in B/Ca and δ11B analyses onto DIC system estimates. Horizontal lines denote seawater concentrations and are calculated from observations of pH and total alkalinity in Jarvis Island benthic reefwater29 and DIC and total alkalinity in Hawaii reefwater33.

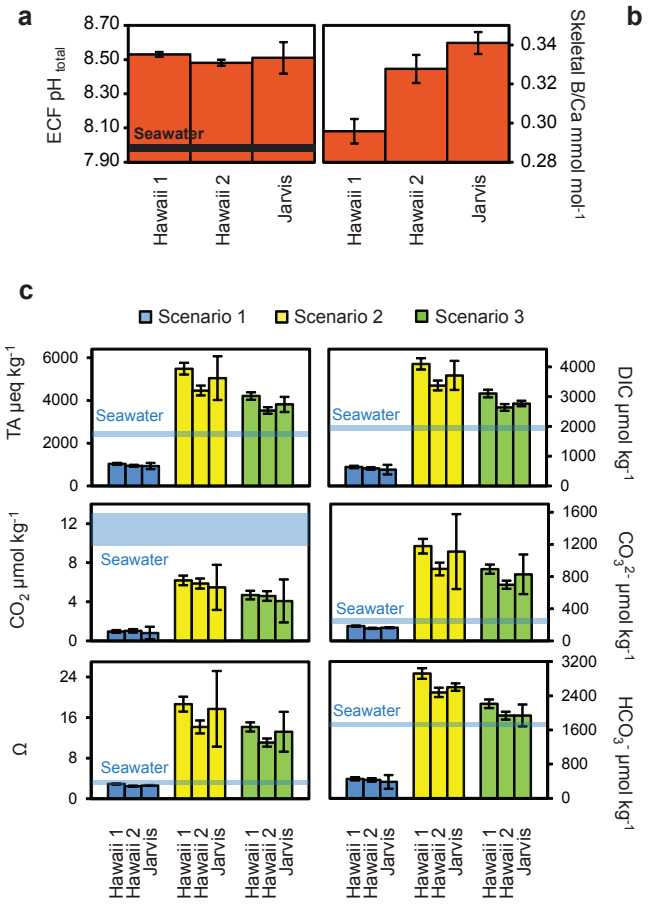

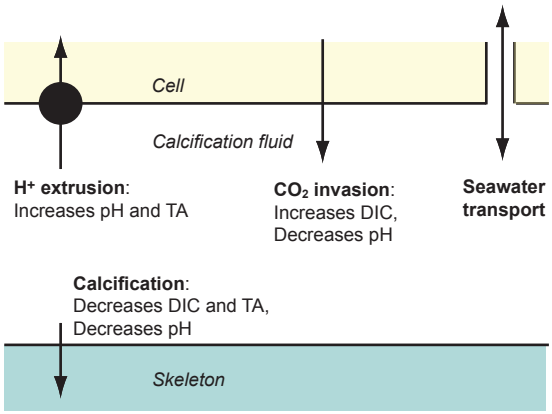

Figure 2. Schematic summarising the processes affecting the DIC system in the coral calcification fluid. The DIC composition reflects the balance of inputs and outputs, namely seawater diffusion, molecular CO2 invasion, proton extrusion and calcification.

Figure 3. Geochemistry and reconstructed calcification fluid DIC of cultured P. damicornis corals. (a) extracellular calcification fluid (ECF) pH (from skeletal δ11B), (b) skeletal B/Ca and (c) reconstructed ECF DIC system parameters. TA = total alkalinity, Ω = aragonite saturation state. Error bars are 95% confidence limits (s.e.m.). Cultured corals were exposed to ruthenium red (RR) dissolved in 0.1% DMSO and DMSO and seawater only controls (con.) were also analysed. Corals were analysed in duplicate (indicated by 1 or 2 annotation). 7-16 analyses were collected on each sample (Table 1) with the exceptions of RR 3.7 μM 2 and RR 5.3 μM 1 where only 2 and 1, respectively, credible δ11B analysis (exhibiting the 42Ca spike throughout the analysis) were obtained. Errors are calculated as for the field corals and horizontal lines denote seawater concentrations calculated from observations of pH and total alkalinity in the culture seawater22.

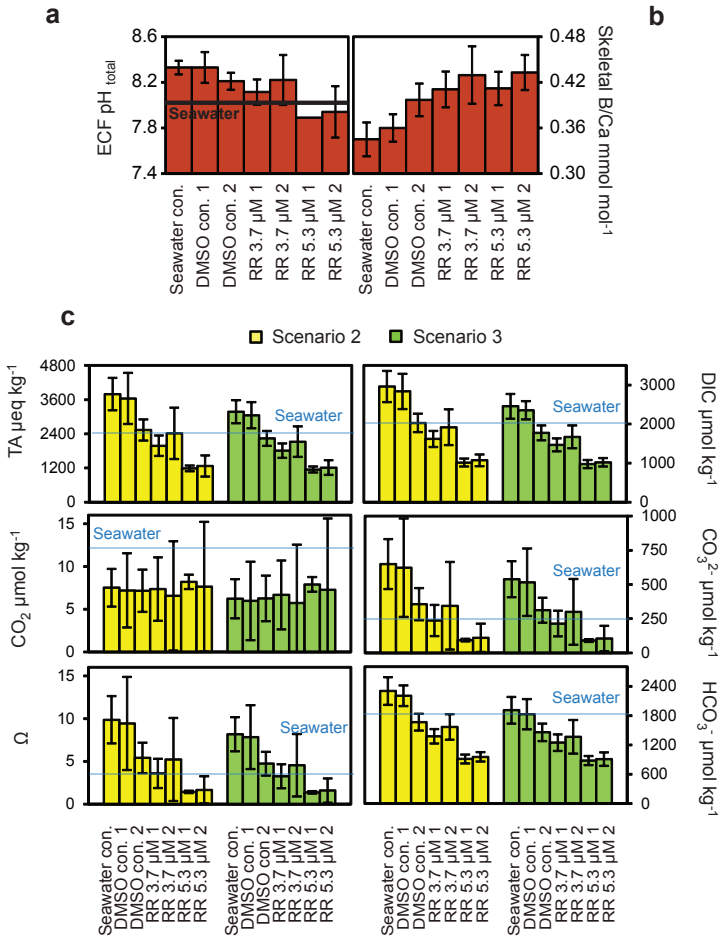

Figure 4. Modelled relationships between calcification fluid pH and DIC parameters under a range of CO2 scenarios. (a) Extracellular calcification fluid (ECF) [DIC] and (b) ECF aragonite saturation state (Ω) increase with ECF pH, assuming that CO2 readily diffuses into the calcification site, maintaining an equilibrium with an overlying [CO2] ranging from that of ambient seawater to 1/8 of this. DIC calculations were made using CO2 sys30, assuming seawater T=25°C and S=40.6 i.e. the conditions in the culture seawater. Reconstructed DIC parameters under scenario 3 in the field and cultured corals are overlain on each graph. Field corals grew under different temperatures and salinities but this does not affect the interpretation of these graphs. Error bars are 95% confidence limits (s.e.m.) and in the case of ECF DIC are smaller than the heights of the symbols.

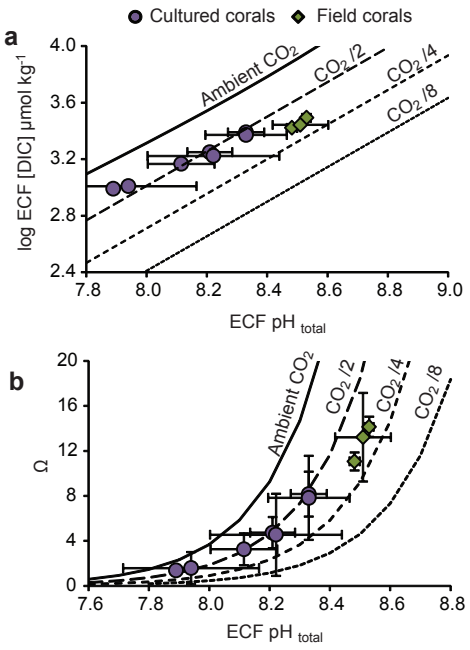

Figure 5. Correlation between reconstructed calcification fluid aragonite saturation state and colony calcification rate in the cultured corals. Aragonite saturation state (Ω) was calculated under scenario 3. Calcification rate is calculated from the mean calcification rate measured in the presence of the inhibitor, if used, as a proportion of the calcification rate observed on day 1, before the introduction of the inhibitor22

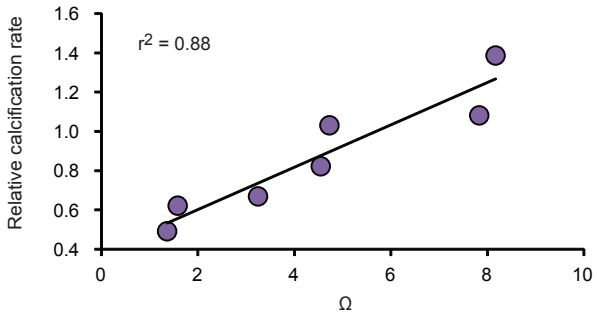

Analysis	B/Ca (mmol mol^{-1})	$\delta^{11}B$ (‰)	Fluid pH_{total}	Partition coefficient x 10^{-3}		
				$B(OH)_4^-/CO_3^{2-}$	$B(OH)_4^-/HCO_3^-$	$B(OH)_4^-/(CO_3^{2-} + HCO_3^-)$
1	0.138	23.4	8.46			
2	0.181	19.8	8.21			
3	0.167	21.0	8.30			
4	0.115	15.1	7.71	0.283	4.51	4.79
5	0.140	17.2	7.98			
6	0.116	20.0	8.23			

Supplementary Table 1. Measured B/Ca and $\delta^{11}B$ in secondary aragonite cements in a Hawaiian fossil coral dated to 13.4ky and estimated pore fluid pH (from $\delta^{11}B$). One analysis (4) formed under a fluid pH of 7.71, close to that observed in modern coral pore fluids (pH = 7.62) which have a a porewater total alkalinity of 2162 ± 78 µmol kg^{-1} (n=4) [1]. We used the B/Ca of this analysis to calculate borate/DIC partition coefficients. Porewater [Ca] is similar to adjacent reefwaters (within 5%) and we assume that porewater [B] is the same as seawater (416 µmol kg^{-1}) at the collection site of the fossil coral and estimate the $[B(OH)_4^-]$ at this fluid pH. We estimate pore fluid $[CO_3^{2-}]$ and $[HCO_3^-]$ from pore fluid pH and total alkalinity using CO2.sys (ref 2) using acidity constants K_1 and K_2 from Roy et al., (ref 3) and $KHSO_4$ from Dickson (ref 4) and assuming T= 25°C and S=35.

References

1. Enmar, R., et al. Diagenesis in live corals from the Gulf of Aqaba. I. The effect on paleo-oceanography tracers, *Geochim. Cosmochim. Acta*, **64**, 3123-3132 (2000).
2. Pierrot, D. E. Lewis, D., & Wallace W.R. MS Excel Program Developed for CO_2 System Calculations. ORNL/CDIAC-105a, Carbon Dioxide Information Analysis Center, Oak Ridge National Laboratory, U.S. Department of Energy, Oak Ridge, Tennessee (2006).
3. Roy RN, Roy LN, Vogel KM, Porter-Moore C, Pearson T, Good, CE, Millero FJ, Campbell DM, The dissociation constants of carbonic acid in seawater at salinities 5 to 45 and temperatures 0 to 45°C, *Mar. Chem.*, **44**, 249-267, (1993).
4. Dickson, A. G., Standard potential of the reaction: AgCl2(s) + 1/2H2(g) = Ag(s) + HCl(aq), and the standard acidity constant of the ion HSO4 in synthetic seawater from 273.15 to 318.15 K., *J. Chem. Thermodyn*. **22**, 113–127 (1990).